Application of radiative renormalization to strong-field resonant nonlinear optical interactions

O. Blum, P. Harshman, and T. K. Gustafson
Department of Electrical Engineering and Computer Sciences and The Electronics Research Laboratory, University of California, Berkeley, California 94720

P. L. Kelley*
Lincoln Laboratory, Massachusetts Institute of Technology, Lexington, Massachusetts 02173
(Received 11 May 1992; revised manuscript received 1 December 1992)

The Liouville equation for the density matrix can be recast so that the external-field terms which couple density-matrix elements are second order in the field. This approach is shown to have a profound effect on the steady-state analysis of strong-field resonant nonlinear optical problems. First, in the case where parity or appropriate field restrictions apply, there is a reduction of the number of coupled equations which must be solved by at least a factor of 2. Second, this reformulation naturally leads to radiative-renormalization terms which are directly related to saturation, Stark shifts, and Rabi splittings. We can use this simple formalism to obtain solutions to a number of resonant nonlinear problems including cases where there are two or more strong fields. The renormalization described here is equivalent to a Dyson-equation analysis.

PACS number(s): 42.65.−k, 42.50.Hz, 32.80.−t

I. INTRODUCTION

Strong-field nonlinear optical interactions have received attention for a variety of reasons, including recent experiments on electromagnetically induced transparency [1, 2] which can occur in a spectral range of strong resonantly enhanced nonlinearity [3]. Strong-field effects include saturation, Stark shifting, Rabi splitting, a strong-field-induced extra resonance, strong-field-induced gain and loss, and "lasers without inversion." For strong fields which are near resonances, conventional perturbation series can diverge and thus give meaningless results. While the coupled equations for the relevant density-matrix elements have been solved in many cases, this process can become extremely complex and cumbersome even in the steady state. For example, if two frequencies are applied to a two-level system, an infinite set of coupled equations arise. If only one field effectively couples pairs of levels in an n-level system, the number of coupled equations is n^2-1. Using a straightforward determinantal solution leads to $(n^2-1)\times(n^2-1)$ determinants which consist of a sum of $(n^2-1)!$ terms. For the three-level problem this leads to 8! or 40 320 terms. For such problems, Gauss elimination usually is used to reduce the number of equations. As shall be seen, the radiative-renormalization method we use leads to multiple Gauss elimination in one step.

It is instructive to consider how the strong-field problem relates to the perturbation approach normally used in nonlinear optics. For some simple cases, the perturbation series have been summed to analytically continue the results to the strong-field limit [4, 7] using Feynman diagram techniques [4–6]. One example is the diagrammatic calculation of the density-matrix element associated with the polarization induced in a two-level system by a single strong, resonant, and continuous radiation field. This calculation demonstrates the basic equivalence of the summing technique with the result obtained by directly solving the coupled equations for the two-level model. In addition, the sum of all perturbation propagators and vertices (diagrams) for the density matrix element can be represented by a Feynman diagram topologically equivalent to the weak-field or lowest-order perturbation diagram (bare diagram), but with the field-independent propagator replaced by a field-dependent or dressed propagator. This field-dependent or dressed propagator is, in lowest order, bilinear in the field.

In this paper, we develop radiative renormalization by using the particularly simple approach of iterative replacement in the density matrix so that the resulting density-matrix equation is of a form where the coupling between the elements is bilinear in the field [8]. If the unperturbed states have parity, there results two sets of density-matrix elements where the elements of one set have been eliminated from the equations for the other set. Thus the replacement process also involves a multifold Gauss elimination. One set (the dipole set) involves those matrix elements for dipole transitions while the other set (the diagonal set) consists of the remaining elements including the diagonal elements. This second set may be reduced by one using the trace invariance. For n even there are $n^2/2$ in the first set and $(n^2-2)/2$ in the second set while for n odd there are $(n^2-1)/2$ in both sets. For the three-level case there are four elements in each set; thus the determinantal solution involves determinants with 4! or 24 elements. This is in contrast

 ©1993 The American Physical Society

to the case described in the first paragraph, i.e., before the elimination was carried out; clearly, a considerable simplification has occurred. Solving one set of equations solves the other since the solutions for one set can be obtained from the other set by substitution in linearly coupled equations. Even if the states do not have parity the number of resonant fields can be chosen so that the iterative replacement process also leads to elimination.

Beside the simplification inherent in this process, it also should be apparent that the bilinear terms which couple a matrix element to itself are radiative renormalizations which lead to saturation, Rabi splitting, and other strong-field processes. While this gives one-photon renormalization, we must carry out higher-order renormalization to include effects such as two-photon saturation. The radiative-renormalization technique described here offers a systematic approach to strong-field excitation problems. In a number of cases one or more frequency components of the field is strong while the other components are weak. In this case, the strong fields may be treated using renormalization while the weak fields are treated using perturbation theory.

In addition to the development of the formal theory of radiative renormalization, as an example we calculate the polarization induced in a two-level system with two strong resonant fields, one of which is the probe, and, in the weak probe limit, show a field-induced extra resonance. We have also applied this technique to three- [9] and four- [10] level systems. For the three-level system we have carried out higher-order (two-photon) renormalization to obtain exact solutions for strong resonant fields connecting both transitions. In the case of a four-level system, we also have obtained exact solutions and have deduced expressions for both third-order sum frequency generation and sum frequency absorption in the presence of two strong fields connecting different pairs of unpopulated levels including two strong-field Rabi splittings. The technique reported here bears a relation to the work of Swain [11]; Osman and Swain have applied these methods to double [12] and triple [13] resonance. We have not yet made a detailed comparison of the two approaches.

II. USE OF THE OPTICAL BLOCH EQUATIONS

Our calculations are based on the use of modified Bloch equations [14] for the density operator. It is important to establish these equations on as firm a footing as possible and to understand their range of validity. The Bloch equations can be obtained through a series of approximations starting from the following generalized model: we consider a "closed" system which has two parts: (1) a subsystem of interest (SOI), which interacts with strong, classical, externally applied electromagnetic fields, and (2) the residual subsystem (RSS), which, as discussed below, we take to be a "heat bath." The interaction between the subsystems requires that we treat the evolution of either subsystem using density matrices since Hamiltonian quantum mechanics is no longer appropriate. We may thus speak of the total system as closed in the sense that its behavior is described by a Hamiltonian while the subsystems are "open" (i.e., they interact with each other) and their evolution is not solely determined by the individual subsystem Hamiltonians. The SOI is typically a group of electronic, vibronic, or orientational states in an atom, molecule, or solid. We treat the interaction of the SOI with unoccupied modes of the radiation field (i.e., the process which leads to spontaneous emission) as part of the RSS interaction. The RSS interaction can also arise from collisions in the case where the SOI is an atom or molecule in a gas or from electron-phonon interaction in the case where the SOI is a lattice electron in a solid.

The development of the model involves deriving equations of motion for the density matrix of the SOI from the evolution equations for the total system (for a discussion of the many aspects of this problem see Refs. [15–21] as well as further references contained in these articles). The SOI density operator equation (sometimes called a "master equation") contains a part which describes the SOI evolution in the external classical field in the absence of the RSS and another term which describes the effect of the RSS on the SOI. The form of this interaction term is quite complex and it is often difficult to make further progress unless physically reasonable simplifying approximations can be made. The interaction term is, in general, nonlocal in time (non-Markovian), involves the interaction between the subsystems to all orders, and depends on the effect of the external classical field on the SOI. In most models the RSS is taken to be a heat bath in the sense that there is a large number of degrees of freedom and it is assumed that the interaction of the SOI with the external field does not perturb the bath sufficiently from equilibrium that it in turn effects the bath interaction with the SOI. Another important assumption, one which is valid for many situations encountered experimentally, is to take the interaction to be weak in the sense that the interaction term can be taken in the lowest-order Born approximation, thus leading to an interaction term which is bilinear in the SOI-bath interaction Hamiltonian. However, for the purpose of the discussion below, it is to be noted that it is not always necessary to neglect, in the interaction terms between the subsystems, the evolution of the SOI due to the external field.

In this paper, we will make the further assumptions that the correlation time for the SOI-bath interaction is short compared to the inverse flopping frequency and the inverse of interaction term itself (i.e., the relaxation time). Note that the flopping frequency involves both the detuning from resonance and the Rabi frequency $\mu E/\hbar$, where μ is a transition dipole and E is the external electric field. In the case of gas collisions, we identify the correlation time with the time duration of an individual collision. The resulting equations have the basic form of the Bloch equations [14] and have important aspects which make further analysis more tractable. The interaction terms are time independent and are "diagonal" in the sense that they couple a density-matrix element ρ_α with itself and, in the case of a diagonal element, with other diagonal elements. Here α represents the matrix

element index pair $\{i,j\}$, where i and j denote energy eigenstates of the SOI without the classical driving fields. In general, the interaction terms are complex quantities with real and imaginary parts which correspond to damping and shifts of transition frequencies. The presence of damping terms indicates irreversibility over some time scale (times short compared to the Poincaré time). The inclusion of the interaction terms in the propagator for the SOI density operator is equivalent to renormalization with respect to collisions. The damping terms for the diagonal elements of the density matrix arise from nonadiabatic processes involving changes of energy while the terms for off-diagonal elements also incorporate adiabatic (i.e., dephasing) processes [22].

The range of validity of the Bloch equations has been the subject of extensive research [15–21, 23]. Important cases lie outside the range of the approximations described in the preceding paragraph; these cases include some aspects of motional narrowing [24, 19] and optically switched collisions [25]. It is possible to apply the approach to generating a master equation for the SOI, as described above, to analyze these cases if less restrictive approximations are made than those leading to the Bloch equations. This, however, is beyond the scope of the present work.

A somewhat different approach than the one taken here is to use the "dressed-atom" picture. The fully quantized dressed-atom picture involves, in the two-level case, considering the mixing, through the atom-radiation interaction, the degenerate (or near-degenerate) atom in the excited state with n photons and atom in the lower state with $(n+1)$ photons [26]. In the semiclassical picture, the equivalent approach is to make the rotating-wave approximation and to perform a time-dependent unitary transformation [27, 22, 28, 29] so that the Hamiltonian becomes time independent; this transformation is possible for multilevel systems where transitions are near resonant with only one frequency component of the field. In a closed system the problem is then reduced to finding the energy eigenvalues and eigenstates and then retransforming eigenstates so that proper expectation values can be calculated. Very near resonance, in the sense that the detuning between the transition frequency and the optical frequency is small compared to the dipolar coupling strength frequency $\mu E/\hbar$, the transformed eigenstates are strong admixtures of the unperturbed states. For an open system, this semiclassical dressed-atom approach may be combined with a SOI master equation derivation [30].

Both radiative renormalization and "dressing" are aimed at the same general goal: a correct description of the behavior of material systems in the presence of strong, resonant electromagnetic fields. However, while the semiclassical dressed-atom approach first solves for the states of the atomic system in the presence of strong radiation fields and then adds interactions with the RSS, the renormalization approach which we develop does the opposite. At least for cases where short correlation approximations cannot be made in the treatment of the heat bath interaction, there is no clear reason to believe that the dressed-atom and radiative-renormalization approaches should lead to different results. More general situations need to be investigated further.

III. GENERAL FORMALISM

The Bloch equation for the density operator $\rho(t)$ of the SOI has the form

$$i\frac{d\rho(t)}{dt} = \frac{1}{\hbar}[H(t),\rho(t)] + \mathcal{R}\rho(t), \tag{1}$$

where $H(t)$ is the Hamiltonian of the SOI including the time-dependent external field and $\mathcal{R}$ is an interaction or "collision" Liouville operator which gives the effect of the heat bath on the SOI and whose properties will be discussed below. We can rewrite Eq. (1) as

$$i\frac{d\rho(t)}{dt} = [\mathcal{L}(t) + \mathcal{R}]\rho(t), \tag{2}$$

where $\mathcal{L}(t)$ is the Liouville operator which is the commutator term divided by $\hbar$. Separating the Liouville operator into the part independent of the external field $\mathcal{L}_0'$ and the field-dependent part $\Omega(t)$, we rewrite the density operator evolution equation once more as

$$i\frac{d\rho(t)}{dt} = [\mathcal{L}_0' + \mathcal{R} + \Omega(t)]\,\rho(t). \tag{3}$$

The Liouville operator $\mathcal{A}$ given by $\mathcal{L}_0'$, $\mathcal{R}$, or $\Omega(t)$ has the matrix form

$$\{\mathcal{A}\rho(t)\}_\alpha = \sum_\beta \mathcal{A}_{\alpha\beta}\rho_\beta(t), \tag{4}$$

where α and β each represent a different pair of state vector quantum numbers $\{i,j\}$. While the i's and j's denote a wave-function basis vector set for the SOI, the α's and β's denote a basis set for matrices belonging to the SOI. It is therefore convenient to consider the density-matrix elements as components of a vector and the Liouville and collision operators as forming matrices in the α space which operate on the density vector [31, 30]. This Liouville space picture is not only a natural consequence of having the system of interest not closed or isolated but instead an open or non-Hamiltonian system, but it also has meaning for isolated systems; consider, for example, the Feynman-Vernon-Hellwarth vector model of the two-level system [32] and its extensions to systems with more than two levels [33, 34].

As a consequence of the short-correlation-time approximations made in deriving the Bloch equation and taking α,β, etc. to belong to the basis set for the external-field-independent part of the Liouville operator $\mathcal{L}_0'$, we have a collision term of the form

$$\{\mathcal{R}\rho(t)\}_{ij} = (1-\delta_{ij})\Gamma_{ij}\rho_{ij}(t) - i\delta_{ij}\left(\Gamma_i^i\rho_{ii}(t) - \sum_{k\ (\neq i)}\Gamma_i^k\rho_{kk}(t)\right) \tag{5}$$

and we take the Γ_{ij}'s and Γ_j^i's to be real and positive; SOI energy-level shifts due to the interaction with the RSS are assumed to be incorporated into $\mathcal{L}_0'$. If the system has a closed population (i.e., the SOI population does not

change), then the trace of Eq. (5) must be zero, which requires the subsidiary conditions $\Gamma_k^k = \sum_{i\neq k}\Gamma_k^i$. We also make the normal statistical physics assumption that $\rho^{(0)}$, the initial value for the density operator before the external field is applied, is diagonal in the energy representation. Detailed balance requires that $\Gamma_i^k\rho_{kk}^{(0)} = \Gamma_k^i\rho_{ii}^{(0)}$ for $i \neq k$.

In addition, for the calculations carried out in this paper, will make the uniform population relaxation assumption

$$\Gamma_i^i\rho_{ii}(t) - \sum_{k\ (\neq i)}\Gamma_i^k\rho_{kk}(t) = \Gamma_d[\rho_{ii}(t) - \rho_{ii}^{(0)}], \tag{6}$$

where Γ_d is the uniform population relaxation constant. In order to obtain this result, we require that $\Gamma_i^i = \Gamma_d(1-\rho_{ii}^{(0)})$ and, for $i \neq k$, $\Gamma_i^k = \Gamma_d\rho_{ii}^{(0)}$. The form of Eq. (6) is valid for any closed population process in a two-level system. It is generally not appropriate for radiative relaxation in multilevel systems. It is apparent that the Bloch equation, as given here, favors the use of the energy representation in the absence of the external field. To simplify subsequent calculations, we combine $\mathcal{L}_0'$ and Γ into a single propagator as follows:

$$\mathcal{L}_0 = \mathcal{L}_0' - i\Gamma, \tag{7}$$

so that the Bloch equation takes on the form

$$i\frac{d\rho(t)}{dt} = [\mathcal{L}_0 + \Omega(t)]\,\rho(t) + i\Gamma_d\rho^{(0)}. \tag{8}$$

Any function of the operator $\mathcal{L}_0$ has the following Liouville space matrix elements in the energy representation:

$$\{f(\mathcal{L}_0)\}_{\alpha\beta} = f((\mathcal{L}_0)_\alpha)\delta_{\alpha\beta}, \tag{9}$$

where

$$\begin{aligned}[\mathcal{L}_0\rho(t)]_\alpha &= \omega_\alpha\rho(t) - i\{\Gamma\rho(t)\}_\alpha \\ &= (1-\delta_{ij})(\omega_{ij} - i\Gamma_{ij})\rho_{ij}(t) - i\delta_{ij}\Gamma_d\rho_{ii}(t).\end{aligned} \tag{10}$$

Here $\omega_\alpha = (\mathcal{L}_0')_\alpha$, i and j are the state vector quantum numbers belonging to α, and $\omega_\alpha = \omega_{ij} = \{(H_0)_{ii} - (H_0)_{jj}\}/\hbar$.

If Eq. (8) is expressed in integral form, it can be written as

$$\begin{aligned}\rho(t) = &\int_{-\infty}^{t} e^{-i\mathcal{L}_0(t-t')}\Omega(t')\rho(t')dt' \\ &+i\Gamma_d\int_{-\infty}^{t} e^{-i\mathcal{L}_0(t-t')}\rho^{(0)}dt'.\end{aligned} \tag{11}$$

The second term on the right-hand side of the equation is an inhomogeneous term associated with the free propagation of the initial density-matrix element. It is important to note that Eq. (11) is not a perturbative result. However, the standard nth-order perturbation result can easily be derived by iterating this equation n times to obtain the density matrix in terms of $n+1$ time integrals of n factors of $\Omega(t)$ multiplying $\rho^{(0)}$.

The expression for the Liouville operator representing the semiclassical interaction of the SOI with the strong external radiation field can be written in the dipole approximation as

$$\begin{aligned}\Omega_{\alpha\alpha'}(\omega) &= \Omega_{i'j'}^{ij}(\omega) \\ &= \mu_{i'j'}^{ij}E(\omega)/\hbar,\end{aligned} \tag{12}$$

where

$$\mu_{i'j'}^{ij} = \mu_{ii'}\delta_{j'j} - \delta_{ii'}\mu_{j'j}. \tag{13}$$

Here $E(\omega)$ is the semiclassical positive analytic signal $e^{-i\omega t}$ and μ_{ij} are the dipole-matrix elements along the direction of polarization. We can also write $\Omega_{\alpha\alpha'}(\omega) = \Omega_{\alpha'\alpha}^*(-\omega)$.

IV. GENERAL APPROACH TO RADIATIVE RENORMALIZATION

As stated in the Introduction, we develop a general approach to radiative renormalization which will provide a straightforward but powerful technique for treating the many strong-field effects which occur in resonant interactions between quantized material systems and semiclassical radiation. Prior analyses have tended to treat these problems in an *ad hoc* unsystematic fashion. By developing the renormalization in a general way we are able to develop an approach which can be readily applied to many problems. We carry out our development in the Fourier transform domain.

The Fourier transform of Eq. (8) is

$$\omega\rho(\omega) = \mathcal{L}_0\rho + \sum_{f_1}\Omega_{f_1}\rho(\omega-\omega_{f_1}) + i\Gamma_d\rho^{(0)}\delta(\omega). \tag{14}$$

Solving for $\rho(\omega)$ gives

$$\rho(\omega) = \frac{1}{\omega-\mathcal{L}_0}\sum_{f_1}\Omega_{f_1}\rho(\omega-\omega_{f_1}) + \rho^{(0)}\delta(\omega). \tag{15}$$

In its simplest form, renormalization involves pairs interaction vertices. To generate such pairs of interactions in density operator equations, a single iteration is carried by rewriting the argument of ρ on the left-hand side of Eq. (15) and substituting this result into the first term on the right-hand side of Eq. (15). The resulting equation,

$$\begin{aligned}&(\omega-\mathcal{L}_0)\rho(\omega) \\ &= \sum_{f_1,f_2}\Omega_{f_2}\frac{1}{\omega-\omega_{f_2}-\mathcal{L}_0}\Omega_{f_1}\rho(\omega-\omega_{f_1}-\omega_{f_2}) \\ &\quad +i\Gamma_d\rho^{(0)}\delta(\omega) + \sum_{f_1}\Omega_{f_1}\rho^{(0)}\delta(\omega-\omega_{f_1}),\end{aligned} \tag{16}$$

has the desired second-order form. The diagonal part of the second-order operator on the density operator can now be combined with the zeroth-order expression on the left-hand side of the equation to give a renormalized-radiative propagator. As has been pointed out in the Introduction, in the typical model of an energy-level transition scheme with parity, this substitution can also pro-

duce a multifold Gauss elimination in a single step which considerably reduces the difficulty of obtaining analytic solutions. If the operators Ω change parity, the second-order terms only connect density operator elements of the same parity. In the two-level case, neglecting for the moment the trace invariance requirement, the four coupled equations for the four density-matrix elements reduce to two sets of two coupled equations, one set for the diagonal terms, the other for the off diagonal terms. Solving one set, for example, the diagonal set, is sufficient since the solutions for the other set may be obtained from the solutions for the first by substitution in Eq. (15). Using the trace invariance simplifies the problem even further as use of this constraint means that only a single equation for a single variable need be solved. Similar reductions in complexity occur for more complex energy-level schemes.

In the generalized relaxation case, we have instead of Eq. (16)

$$(\omega-\mathcal{L}_0)\rho(\omega)=\sum_{f_1,f_2}\Omega_{f_2}\frac{1}{\omega-\omega_{f_2}-\mathcal{L}_0}\Omega_{f_1}\rho(\omega-\omega_{f_1}-\omega_{f_2}). \tag{17}$$

Here $\mathcal{L}_0=\mathcal{L}_0'+\mathcal{R}$ and $\mathcal{R}$ is defined by Eq. (5). To avoid nondiagonal denominators in the renormalization terms, we take Eq. (17) to be an equation for the diagonal set only.

Returning to the uniform relaxation case, the second-order result can be expressed in terms of the components of the density vector and propagator and external field matrices as follows:

$$\rho_\alpha(\omega)=\left(\frac{1}{\omega-\mathcal{L}_0}\right)_\alpha\sum_{f_1,f_2}\left[\left(\Omega_{f_2}\frac{1}{\omega-\omega_{f_2}-\mathcal{L}_0}\Omega_{f_1}\right)_{\alpha\alpha}\rho_\alpha(\omega-\omega_{f_1}-\omega_{f_2})+\sum_{\beta\ (\neq\alpha)}\left(\Omega_{f_2}\frac{1}{\omega-\omega_{f_2}-\mathcal{L}_0}\Omega_{f_1}\right)_{\alpha\beta}\rho_\beta(\omega-\omega_{f_1}-\omega_{f_2})\right]+S_\alpha(\omega). \tag{18}$$

The quantity $S_\alpha(\omega)$ is given by

$$S_\alpha(\omega)=\rho_\alpha^{(0)}\delta(\omega)+\left(\frac{1}{\omega-\mathcal{L}_0}\right)_\alpha\sum_{f_1}\sum_{\delta}(\Omega_{f_1})_{\alpha\delta}\rho_\delta^{(0)}\delta(\omega-\omega_{f_1}). \tag{19}$$

We see that several types of terms involving pairs of interactions arise in the above equations. The first term is diagonal in the sense that it involves the evolution of a density component $\rho_\alpha(\omega-\omega_{f_1}-\omega_{f_2})$ through two interactions with the field to the same density-matrix element $\rho_\alpha(\omega)$, but evaluated at a frequency which is shifted by the difference of the two interaction frequencies. $(\Omega_{f_1})_{\gamma\alpha}$ is the first interaction taking the system from "state" α to an intermediate density operator state, which we define as γ. Further, $1/(\omega-\omega_{f_2}-\mathcal{L}_0)_\gamma$ is the propagator associated with the γ intermediate state, $(\Omega_{f_2})_{\alpha\gamma}$ is the interaction associated with the second vertex bringing the system back to the α state, and $1/(\omega-\mathcal{L}_0)_\alpha$ is the final propagator in the α state. The first set of terms directly renormalize the components of the density vector when $\omega_{f_1}=-\omega_{f_2}$ and provide terms giving saturation, Rabi splitting, etc. The second set of terms in Eq. (18) is associated with a change in the density-matrix element and has a similar interpretation of the coefficients. $S_\alpha(\omega)$ is a source term due to the initial values of the elements of the density vector, the first term in the expression resulting from free propagation and the factor in front, $1/(\omega-\mathcal{L}_0)_\alpha$, once again being the bare propagator for this evolution. The second term in $S_\alpha(\omega)$ gives the evolution to the final element from an equilibrium element through a single interaction.

V. CALCULATION OF POPULATION DIFFERENCES

One important class of nonlinear optical processes involves strong fields connecting only one pair of energy levels. In this case, we can rewrite the equations for the diagonal elements of the two levels in terms of the difference between the density-matrix elements, which we take to be η and ϵ. Introducing the population difference term $\Delta\rho=\rho_\eta-\rho_\epsilon$, we obtain from Eqs. (18) and (19)

$$\begin{aligned}\Delta\rho(\omega)=\frac{1}{\omega+i\Gamma_1}\sum_{f_1,f_2}\Bigg[&\left\{\left(\Omega_{f_2}\frac{1}{\omega-\omega_{f_2}-\mathcal{L}_0}\Omega_{f_1}\right)_{\eta\eta}-\left(\Omega_{f_2}\frac{1}{\omega-\omega_{f_2}-\mathcal{L}_0}\Omega_{f_1}\right)_{\epsilon\eta}\right\}\rho_\eta(\omega-\omega_{f_1}-\omega_{f_2})\\&-\left\{\left(\Omega_{f_2}\frac{1}{\omega-\omega_{f_2}-\mathcal{L}_0}\Omega_{f_1}\right)_{\epsilon\epsilon}-\left(\Omega_{f_2}\frac{1}{\omega-\omega_{f_2}-\mathcal{L}_0}\Omega_{f_1}\right)_{\eta\epsilon}\right\}\rho_\epsilon(\omega-\omega_{f_1}-\omega_{f_2})\\&+\sum_{\alpha\ (\neq\eta,\epsilon)}\left\{\left(\Omega_{f_2}\frac{1}{\omega-\omega_{f_2}-\mathcal{L}_0}\Omega_{f_1}\right)_{\eta\alpha}-\left(\Omega_{f_2}\frac{1}{\omega-\omega_{f_2}-\mathcal{L}_0}\Omega_{f_1}\right)\right\}_{\epsilon\alpha}\rho_\alpha(\omega-\omega_{f_1}-\omega_{f_2})\Bigg]\\&+\Delta\rho^{(0)}\delta(\omega),\end{aligned} \tag{20}$$

where we have replaced Γ_d with the more familiar Γ_1. The first four terms in Eq. (20) which involve only the η and ϵ elements can be represented by 32 Feynman diagrams half of which are shown in Figs. 1 and 2. These and subsequent diagrams are double sided in that the vertical lines represent the propagation of the density-matrix elements and the photon lines have the usual meaning [4–6]. Note that each of those four terms generates eight diagrams when the Liouville operators are expanded so that interactions on both sides of the diagram are shown explicitly. Choosing ω_{f1} as a positive frequency (downward slope, left to right in the figures) and ω_{f2} as negative frequency (upward slope, left to right), as shown in Fig. 1, and also choosing η to be a lower energy state than ϵ makes the upper set of four diagrams resonant in the first propagator occurring between the two interactions $(\frac{1}{\omega-\omega_{f2}-\mathcal{L}_0})$ and also the final propagator $(\frac{1}{\omega+i\Gamma})$ after both interactions. The lower four are nonresonant in the propagator between the two interactions, but remain resonant in the final propagator. The opposite choice for ω_{f1} and ω_{f2} (negative and positive respectively) results in an analogous set of eight diagrams as shown in Fig. 2 with the slopes of the photon lines opposite to that shown in Fig. 1. For these the lower four would be resonant for the same level selection. There are also 16 additional diagrams having both ω_{f1} and ω_{f2} of the same sign, either positive or negative. All of these are nonresonant in the final propagator, but half remain resonant in the first propagator.

One observes that the interaction and propagator factors for the four upper diagrams in Figs. 1(a)–1(d) are equal and those of the lower set of four are equal. Thus combining (a) with (b) and (c) with (d) yields a factor of 2. These can be written as one factor multiplying $\Delta\rho(\omega-\omega_{f1}-\omega_{f2})$. The two resulting terms, one fully resonant and the other nonresonant, will be represented by the collapsed diagram shown in Fig. 1(e). A similar analysis can also be done with Fig. 2. Expressed analytically, Eq. (20) can be more compactly written as

$$\Delta\rho(\omega) = \frac{2}{\omega+i\Gamma_1}\sum_{f_1,f_2}\left(\Omega_{f_2}\frac{1}{\omega-\omega_{f_2}-\mathcal{L}_0}\Omega_{f_1}\right)_{\epsilon\epsilon}\Delta\rho(\omega-\omega_{f_1}-\omega_{f_2}) + \sum_{\alpha\ (\neq\eta,\epsilon)}\left\{\left(\Omega_{f_2}\frac{1}{\omega-\omega_{f_2}-\mathcal{L}_0}\Omega_{f_1}\right)_{\epsilon\alpha} - \left(\Omega_{f_2}\frac{1}{\omega-\omega_{f_2}-\mathcal{L}_0}\Omega_{f_1}\right)_{\eta\alpha}\right\}\rho_\alpha(\omega-\omega_{f_1}-\omega_{f_2}) + \Delta\rho^{(0)}\delta(\omega), \quad (21)$$

where each term in the first sum represents the eight possible diagrammatic contributions. In general the terms on the second line cannot be expressed as propagator terms multiplied by the difference between density matrix elements.

The right-hand side of Eq. (21) includes (1) a term involving the same density-matrix element at the same frequency as the left-hand side, (2) possibly the same element at a shifted frequency, (3) terms involving other density-matrix elements also at shifted frequencies, and (4) a source term involving the equilibrium population.

The equations for the density-matrix elements or their differences can be considerably reduced in number by the above iteration procedure. The solution for a particular population difference can be obtained by the successive elimination of density-matrix elements. Since this involves the array of coefficients of the set of coupled equations, and in particular the diagonalization of this array, this elimination procedure is equivalent to a set of nested

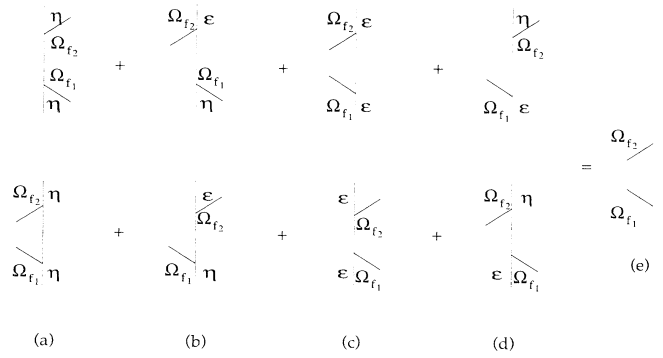

FIG. 1. Diagrams contributing to the first four terms in Eq. (20) for ω_{f1} negative and ω_{f2} positive. In (a) and (b) the initial density-matrix element is $\rho_\eta(\omega-\omega_{f_1}-\omega_{f_2})$ and in (c) and (d), $\rho_\epsilon(\omega-\omega_{f_1}-\omega_{f_2})$. The drawing in (e), defined as the collapsed diagram, will be used to represent all eight double Feynman diagrams. For η the ground state and ϵ the upper state, the four upper diagrams are resonant. The lower four will be dropped from consideration.

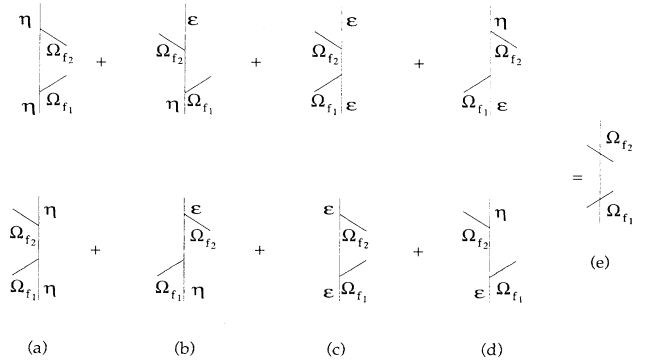

FIG. 2. Diagrams contributing to the first set of terms in Eq. (20) for ω_{f1} positive and ω_{f2} negative. As in Fig. 1, in (a) and (b) the initial density-matrix element is $\rho_\eta(\omega-\omega_{f_1}-\omega_{f_2})$ and in (c) and (d), $\rho_\epsilon(\omega-\omega_{f_1}-\omega_{f_2})$. Also the collapsed diagram in (e) represents all eight double Feynman diagrams. For η the ground state and ϵ the upper state, the four lower diagrams are resonant.

Dyson equations for the coefficients in Eqs. (16) or (18). Thus, once rules are established for this elimination procedure, knowing the weak-field interaction allows one to immediately write down the strong-field result in terms of renormalized coefficients.

In summary, the form of the equations for a given density component involves (1) external-field terms coupling the same density component including a term which does not give a frequency shift and which serves as a first-order renormalization, (2) coupling terms involving other density components, and (3) a source term involving the initial population. The particular approach taken in this section is not very useful for problems where the strong fields do not change populations; in this case, direct, simple solutions may be obtained from Eqs. (16) and (18).

VI. TWO-LEVEL SYSTEM—TWO STRONG FIELDS

As an application of this approach, we consider the two-level system [35–37]. In the present case we take $\Delta\rho = \rho_\eta - \rho_\epsilon = \rho_{11} - \rho_{22}$, where 1 and 2 are the lower and upper states, respectively. Since the trace is equal to unity, one can write $\rho_\eta = \frac{1}{2}(1+\Delta\rho)$ and $\rho_\epsilon = \frac{1}{2}(1-\Delta\rho)$. Assuming for simplicity that the decay rate of the two states is the same, Eq. (21) becomes

$$\Delta\rho(\omega) = \frac{2}{\omega + i\Gamma_1}\sum_{f_1,f_2}\left(\Omega_{f_2}\frac{1}{\omega-\omega_{f_2}-\mathcal{L}_0}\Omega_{f_1}\right)_{\epsilon\epsilon} \times\Delta\rho(\omega-\omega_{f_1}-\omega_{f_2}) + \Delta\rho^{(0)}\delta(\omega), \tag{22}$$

where it is noted that the index pair $\epsilon\epsilon$ could be replaced by the four other possible combinations of η and ϵ since these are all equal as discussed above.

We consider the case of two strong fields at two angular frequencies ν and ν' where both the positive and negative analytic signals at both frequencies are to be considered ($\omega_{f1} = \pm\nu, \pm\nu'$ and similarly for ω_{f2}). Including all possible frequency components $n(\nu'-\nu)$ arising from the mixing of the two signals, the population difference spectral distribution can be written as

$$\Delta\rho(\omega) = \sum_{n=-\infty}^{\infty}\Delta\rho_n\delta(\omega - n(\nu'-\nu)), \tag{23}$$

where $\Delta\rho_n$ is the spectral component at frequency $n(\nu'-\nu)$. These population beat terms have been studied extensively [38]. In general for any combination of assignments $\pm\nu$ and $\pm\nu'$ to ω_{f1} and ω_{f2} there are eight diagrams analogous to those shown in Figs. 1(a)–1(d). Given 16 distinct combinations, a total of 128 diagrams or 16 collapsed diagrams analogous to Fig. 1(e) are possible. However, ω_{f1} and ω_{f2} must have opposite signs to consider the beat terms, thereby eliminating the diagrams with photon lines of the same slope. There remain 64 diagrams, or eight collapsed diagrams, to be considered. If one furthermore restricts the analysis to fully resonant terms [both propagators in Eq. (22)], then each collapsed diagram corresponds to a single term in Eq. (22).

In terms of the spectral components, Eq. (22) can be written in the form

$$\Delta\rho_n = -r_n\Delta\rho_n - a_n\Delta\rho_{n+1} - b_n\Delta\rho_{n-1} + \Delta\rho^{(0)}\delta_{n,0}. \tag{24}$$

The first term in r_n is given by a collapsed diagram of Fig. 1 with $\omega_{f1} = -\nu = -\omega_{f2}$, a second with $\omega_{f1} = \nu = -\omega_{f2}$; in addition, a third and fourth with ν replaced by ν'. Thus r_n is given by

$$r_n = 2d_n\left[|\Omega|^2\left(\frac{1}{n(\nu'-\nu)-\nu+\omega_0+i\Gamma_2}+\frac{1}{n(\nu'-\nu)+\nu-\omega_0+i\Gamma_2}\right) + |\Omega'|^2\left(\frac{1}{n(\nu'-\nu)-\nu'+\omega_0+i\Gamma_2}+\frac{1}{n(\nu'-\nu)+\nu'-\omega_0+i\Gamma_2}\right)\right], \tag{25}$$

which is diagrammatically represented as shown in Fig. 3. Similarly a_n in Fig. 3 is given analytically by

$$a_n = 2d_n\Omega'^*\Omega\left(\frac{1}{n(\nu'-\nu)-\nu+\omega_0+i\Gamma_2} + \frac{1}{n(\nu'-\nu)+\nu'-\omega_0+i\Gamma_2}\right). \tag{26}$$

Here $\omega_{f1} = -\nu'$ and $\omega_{f2} = \nu$ for the first term and $\omega_{f1} = \nu$ and $\omega_{f2} = -\nu'$ for the second term. b_n is obtained by interchanging ν and ν' in a_n. Thus

$$b_n = 2d_n\Omega^*\Omega'\left(\frac{1}{n(\nu'-\nu)+\nu-\omega_0+i\Gamma_2} + \frac{1}{n(\nu'-\nu)-\nu'+\omega_0+i\Gamma_2}\right). \tag{27}$$

In all of these the d_n factor is given by

$$d_n = \frac{-1}{n(\nu'-\nu)+i\Gamma_1}. \tag{28}$$

Also, $\omega_0 = \omega_{21}$, $\Gamma_2 = \Gamma_{21}$, $\Omega = \mu_{21}E(\nu)/\hbar$, and $\Omega' = \mu_{21}E(\nu')/\hbar$.

The resulting equations for $\Delta\rho_n$ consist of a set of coupled equations, which can be solved by elimination. To do this we first write the equations in the form

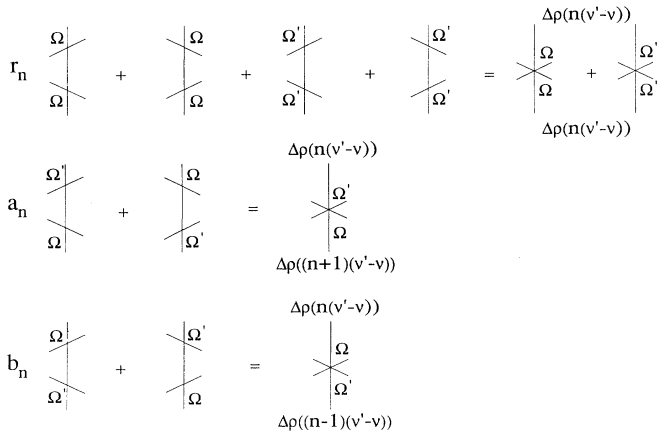

FIG. 3. Diagrams of the renormalization and coupling terms for the spectral components of the population difference of a two-level system with two strong fields. The initial spectral components are shown below the diagrams representing the overall processes while the final spectral components are shown above the diagrams. r_n is the self-renormalization component and a_n and b_n the population beat components.

$$\Delta\rho_n + A_n\Delta\rho_{n+1} + B_n\Delta\rho_{n-1} = \frac{1}{1+r_n}\Delta\rho^{(0)}\delta_{n,0}, \tag{29}$$

where $A_n = a_n/(1 + r_n)$ and $B_n = b_n/(1 + r_n)$ are the propagator coefficients renormalized by absorption-emission processes at the same frequency, that is, the diagonal, or self-renormalized, components in the frequency domain.

To solve the set of equations for positive values of n, let $\Delta\rho_{n+1} = -\hat{B}_{n+1}\Delta\rho_n$, where $\hat{B}_{n+1}$ is the renormalization of B_{n+1} by terms where the value of the index is greater than $n + 1$. Using this expression in Eq. (29) we obtain an equation which generates $\Delta\rho_n$ in terms of $\Delta\rho_{n-1}$,

$$\Delta\rho_n - A_n\hat{B}_{n+1}\Delta\rho_n + B_n\Delta\rho_{n-1} = 0. \tag{30}$$

Substituting $\Delta\rho_n = -\hat{B}_n\Delta\rho_{n-1}$ and solving for $\hat{B}_n$,

$$\hat{B}_n = \frac{B_n}{1 - A_n\hat{B}_{n+1}}. \tag{31}$$

Successive resubstitution for the $\hat{B}_n$'s generates the continued fraction expansion

$$\hat{B}_n = \cfrac{B_n}{1 - \cfrac{A_nB_{n+1}}{1 - \cfrac{A_{n+1}B_{n+2}}{1 - \cdots}}}, \tag{32}$$

when n is positive. This fraction may be truncated at an appropriate point when the A_n and B_n become smaller with increasing n. A similar set of equations is obtained for negative integers; introducing $\Delta\rho_{n-1} = -\hat{A}_{n-1}\Delta\rho_n$, we find

$$\hat{A}_n = \cfrac{A_n}{1 - \cfrac{B_nA_{n-1}}{1 - \cfrac{B_{n-1}A_{n-2}}{1 - \cdots}}}, \tag{33}$$

when n is negative. Since $A_{-n} = B_n^*$ for all n, the expansion for positive integers is the complex conjugate of the expansion for negative integers. Such continued-fraction expansions have been used in strong-field two-level problems to analyze (1) the single frequency case without making the rotating-wave approximation [39], (2) standing-wave effects in Doppler broadened systems [40, 41], and (3) the case of two independent strong fields [42, 43]. The last two cases are treated in the present analysis.

For $n > 0$, the expression for $\Delta\rho_n$ in terms of $\Delta\rho_0$ is

$$\Delta\rho_n = (-1)^n\Delta\rho_0\prod_{m=1}^{n}\hat{B}_m, \tag{34}$$

where

$$\Delta\rho_0 = \left(\frac{1}{1 - A_0\hat{B}_1 - A_0^*\hat{B}_1^*}\right)\frac{1}{1+r_0}\Delta\rho^{(0)} \tag{35}$$

from Eq. (29) and it is noted that $\Delta\rho_{-n} = \Delta\rho_n^*$.

The dipolar density-matrix elements at frequency ω is given by

$$\rho_{21}(\omega) = \sum_n \rho_{21,n}\delta(\omega - \nu - n(\nu' - \nu)). \tag{36}$$

We use Eq. (15) and substitute the diagonal elements $\Delta\rho_n$ and $\Delta\rho_{n+1}$ on the right-hand side to obtain the Fourier coefficients

$$\rho_{21,n} = \frac{1}{\nu + n(\nu' - \nu) - \omega_0 + i\Gamma_2}\left[\Omega'\Delta\rho_{n-1} + \Omega\Delta\rho_n\right]. \tag{37}$$

The diagrammatic representation of these terms is shown in Fig. 4. It is apparent that there are multiple resonances in ν' which occur at ν and $\nu + (\omega_0 - \nu)/n$. These subharmonic resonances are well known in nonlinear optics.

The dipolar density-matrix-element coefficient at frequency ν' is given by setting $n = 1$ in Eq. (37),

$$\begin{aligned}\rho_{21,1} &= \frac{1}{\nu' - \omega_0 + i\Gamma_2}\left[\Omega'\Delta\rho_0 + \Omega\Delta\rho_1\right] \\ &= \frac{1}{\nu' - \omega_0 + i\Gamma_2}\left[\Omega' - \Omega\hat{B}_1\right] \\ &\quad\times\left(\frac{1}{1 - A_0\hat{B}_1 - A_0^*\hat{B}_1^*}\right)\frac{1}{1+r_0}\Delta\rho^{(0)}.\end{aligned} \tag{38}$$

A. Dyson-equation picture

Equation (31) is equivalent to a Dyson equation, which is apparent by expressing the equation in the form $\hat{B}_n = B_n + A_n\hat{B}_{n+1}\hat{B}_n$. Thus the strong-field-limit term $\hat{B}_n$

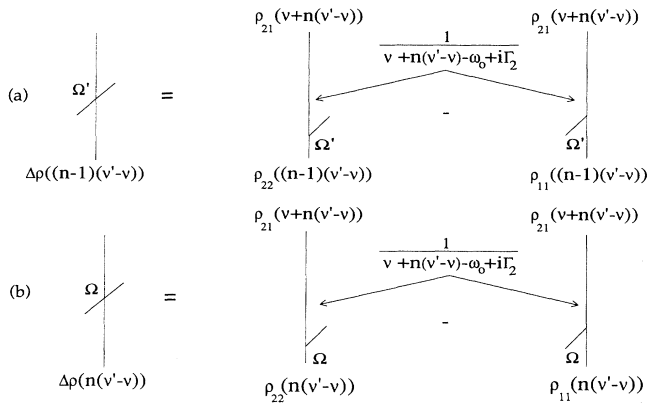

FIG. 4. The diagrams giving the dipolar density-matrix element $\rho_{21,n}$ as given by Eq. (37). The collapsed diagrams shown in (a) and (b), which couple $\rho_{21,n}$ with $\Delta\rho_{n-1}$ and $\Delta\rho_n$, respectively, are given by the sum of two diagrams. (a) corresponds to the first term of Eq. (37) and (b) to the second term of Eq. (37).

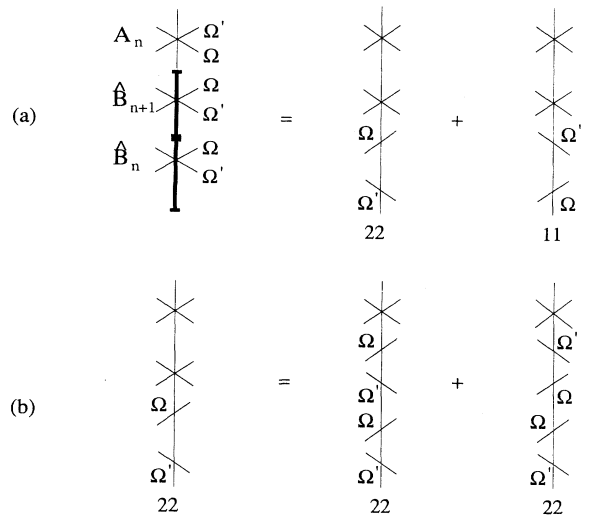

FIG. 5. The terms contributing to the triple-product terms $\hat{B}_n\hat{B}_{n+1}A_n$ in the Dyson equation for $\hat{B}_n$. Thick lines are used to represent strong-field terms, and thin lines, weak-field terms. (a) shows the eight terms which result when the first cross vertex is expanded. The first of these is expanded further in (b) by expanding the second cross vertex showing that each term of (a) results in four further resonant terms with this expansion.

is given by the sum of the weak-field-limit term and a strong-field contribution, the latter being the product of the strong-field-limit term itself, the strong-field-limit term $\hat{B}_{n+1}$ and the weak-field-limit term $\hat{A}_n$, which is the usual Dyson relationship. The strong-field-limit term can be interpreted as arising from the strong-field-limit excitation of $n(\nu-\nu')$ from the strong-field-limit $(n-1)(\nu-\nu')$ excitation, followed by the strong-field-limit excitation of $\Delta\rho_{n+1}$ by $\hat{B}_{n+1}$ operating on $\Delta\rho_n$ and its subsequent destruction by the weak-field-limit term A_n which brings the excitation back to $n(\nu-\nu')$. $\hat{B}_{n+1}$, the strong-field-limit term in the Dyson equation, is in turn given by an analogous relationship, with n replaced by $n+1$, thereby leading to a nested relationship which is equivalent to the continued fraction expansion.

The proliferation of double Feynman terms contributing to the triple product term of the Dyson relation can be illustrated by considering the lowest-order contribution, which is $A_nB_{n+1}B_n$. This includes the spectral self-renormalization. This is shown in Fig. 5 where thick lines are used to represent $\hat{B}$. B_n has the two resonant collapsed terms of Fig. 3(c) or Eq. (27) arising in turn from eight resonant diagrams. To be resonant the subsequent B_{n+1} factor can only correspond to the same collapsed diagram as the corresponding B_n to be resonant, thus multiplying the number of double diagrams by 4. This is also true for the A_n factor resulting in two collapsed terms arising from 128 double diagrams. The reduction in the 128 diagrams to 2 using the population difference $\Delta\rho$ and the assumption $\Gamma_{11}=\Gamma_{22}$ is quite apparent.

The analysis of $\Delta\rho_0$ in terms of Dyson equations is simpler in that in the lowest order of approximation $\Delta\rho_0=\Delta\rho^{(0)}$, so that the counting of the terms simply starts with the next higher order, with the number of diagrams being 4×4 coming from the creation of an $\nu'-\nu$ excitation followed by its destruction. With the approximation $\Gamma_{11}=\Gamma_{22}$, this number is once again reduced by 2×2, thus coinciding with the number of factors coming from A_0 and B_1.

B. Application to the Doppler effect

The response of a distribution of moving atoms to a standing-wave optical field may be analyzed by assuming that ν and ν' are the frequencies, in the rest frame of the moving atoms, of the oppositely directed traveling-wave components of a standing-wave field along the z axis. Assuming the ν field propagates in the $+z$ direction and ν' field propagates in the $-z$ direction, we have, for an atom moving with velocity $v_z=v$,

$$\nu=\bar{\nu}-kv,$$

$$\nu'=\bar{\nu}+kv,$$

where $\bar{\nu}$ is the frequency of the field in the laboratory frame and k is the propagation constant.

The Fourier spectrum of the dipolar term is given by

$$\rho_{21}(\omega)=\frac{1}{\sqrt{\pi}v_{\rm th}}\int dv\, e^{-v^2/v_{\rm th}^2}\rho_{21}(\omega,v), \tag{39}$$

where the thermal velocity $v_{\rm th}=\sqrt{kT/M}$ and

$$\rho_{21}(\omega,v)=\sum_n \rho^d_{21,n}\delta(\omega-\bar{\nu}-(2n-1\pm 1)kv). \tag{40}$$

The ± 1 term in the δ function comes from the transformation of the polarization generated by the atoms back into the laboratory frame. The + sign is for the polarization wave traveling in the $+z$ direction and the − sign is for the polarization wave traveling in the $-z$ direction. The Fourier coefficients are given by

$$\rho^d_{21,n}=\frac{1}{\bar{\nu}+(2n-1)kv-\omega_0+i\Gamma_2}\left[\Omega'\Delta\rho^d_{n-1}+\Omega\Delta\rho^d_n\right]. \tag{41}$$

The population differences $\Delta\rho^d_n$ are in turn given by Eqs. (34) and (35), but with the a_n, b_n, r_n, and d_n in the expressions for the A_n's and B_n's replaced by

$$r^d_n=2d^d_n\left[|\Omega|^2\left(\frac{1}{(2n+1)kv-\bar{\nu}+\omega_0+i\Gamma_2}+\frac{1}{(2n-1)kv+\bar{\nu}-\omega_0+i\Gamma_2}\right)\right.$$
$$\left.+|\Omega'|^2\left(\frac{1}{(2n-1)kv-\bar{\nu}+\omega_0+i\Gamma_2}+\frac{1}{(2n+1)kv+\bar{\nu}-\omega_0+i\Gamma_2}\right)\right], \tag{42}$$

$$a^d_n=2d^d_n\Omega'^*\Omega\left(\frac{1}{(2n+1)kv-\bar{\nu}+\omega_0+i\Gamma_2}+\frac{1}{(2n+1)kv+\bar{\nu}-\omega_0+i\Gamma_2}\right), \tag{43}$$

$$b^d_n=2d^d_n\Omega^*\Omega'\left(\frac{1}{(2n-1)kv+\bar{\nu}-\omega_0+i\Gamma_2}+\frac{1}{(2n-1)kv-\bar{\nu}+\omega_0+i\Gamma_2}\right), \tag{44}$$

and

$$d^d_n=\frac{-1}{2nkv+i\Gamma_1}. \tag{45}$$

Since we have not assumed that the field amplitudes are equal, these results are more general than for the true standing-wave case.

There are two general classes of terms in the Fourier spectrum. The first class occurs either when $n=0$ for the $+z$ polarization wave or when $n=1$ for the $-z$ polarization wave. These terms have sharp Fourier components at $\omega=\bar{\nu}$, are spatially phase matched to the field, and contain contributions from all velocity groups but weighted by velocity resonances which occur in a_n, b_n, r_n, and d_n. For these terms, it is apparent that the velocity groups at $v=0$ and $v=(\omega_0-\bar{\nu})/(2m+1)k$ (where m takes on any integer value) are most strongly affected by the field [44, 45]. The remainder of the terms in the Fourier spectrum form the second class in which the polarization waves have spatial frequencies that are much higher than those of the resonant field. In this class, each atomic velocity contributes a different frequency component and, despite the fact that the excitation spectrum is monochromatic, a broadened polarization spectrum results which is weighted by the resonances in a_n, b_n, r_n, and d_n.

C. Single strong-field limit

The limit in which one field is a weak probe which can be treated perturbatively is of interest because of its relevance to saturation spectroscopy and inversionless gain. This limit also allows further insight into the basic renormalization process. Furthermore, extensions of this approach to situations in which numerous strong fields are present in multilevel systems are useful.

For a strong field at ν, the pump, and a weak-field probe at ν', we find that, for $n>0$, the leading term in $\Delta\rho_n$ is

$$\Delta\rho_n=(-1)^n\Delta\rho_0\prod_{m=1}^{n}B_m, \tag{46}$$

where

$$\Delta\rho_0=\frac{1}{1+r_0}\Delta\rho^{(0)}, \tag{47}$$

$$r_n=2d_n|\Omega|^2\left(\frac{1}{n(\nu'-\nu)-\nu+\omega_0+i\Gamma_2}+\frac{1}{n(\nu'-\nu)+\nu-\omega_0+i\Gamma_2}\right), \tag{48}$$

and all the other quantities are defined as before. Note that there are no longer continued-fraction expressions. If both fields are weak, then $r_n=0$ and B_m is replaced by b_m in Eq. (46).

The leading terms in the Fourier coefficients of the dipolar density-matrix elements are given in the weak probe-field limit by

$$\rho_{21,n}=\begin{cases}\dfrac{1}{\nu+n(\nu'-\nu)-\omega_0+i\Gamma_2}\left[\Omega'\Delta\rho_{n-1}+\Omega\Delta\rho_n\right], & n\geq 1\\ \dfrac{1}{\nu+n(\nu'-\nu)-\omega_0+i\Gamma_2}\Omega\Delta\rho_n, & n\leq 0.\end{cases} \tag{49}$$

D. Linear response to the weak field

There are two frequency components which are linear in the weak field, one at ν' and the other at $2\nu - \nu'$. The first is the Stokes response while the second is the phase-conjugated four-wave mixing or anti-Stokes response. Setting $n = 1$ in Eq. (49), and correspondingly in Fig. 4, and substituting $\Delta\rho_1 = -B_1\Delta\rho_0$, the Stokes Fourier component at ν' is given by

$$\rho_{21,1} = \frac{-i}{D_2}\left[\Omega' - \Omega B_1\right]\Delta\rho_0. \tag{50}$$

Both Figs. 4(a) and 4(b) contribute terms in this linear approximation. The anti-Stokes Fourier component at $2\nu - \nu'$ is obtained by setting $n = -1$ in Eq. 49 and in Fig. 4. In this case since $\Delta\rho_{-2} = -B_2^*\Delta\rho_{-1}$, which is higher order in Ω'^*, so that the processes of Fig. 4(a) can be neglected. Thus the linear response at $2\nu - \nu'$ is

$$\rho_{21,-1} = \frac{i\Omega B_1^*\Delta\rho_0}{D_4^*}, \tag{51}$$

where we have substituted $\Delta\rho_{-1} = -B_1^*\Delta\rho_0$. In these equations

$$\Delta\rho_0 = \frac{1}{1 + \frac{4|\Omega|^2\Gamma_2}{|D_3|^2\Gamma_1}}\Delta\rho^{(0)} \tag{52}$$

and

$$\begin{aligned}\frac{\Omega B_1}{\Omega'} &= \frac{\Omega b_1}{\Omega'(1+r_1)} \\ &= \frac{-i2d_1|\Omega|^2}{1+r_1}\left(\frac{1}{D_2} + \frac{1}{D_3}\right) \\ &= \frac{2|\Omega|^2 D_4(D_2+D_3)}{D_3[D_1D_2D_4 + 2|\Omega|^2(D_2+D_4)]}.\end{aligned} \tag{53}$$

Also,

$$\begin{aligned}D_1 &= i(\nu - \nu') + \Gamma_1, \\ D_2 &= i(\omega_0 - \nu') + \Gamma_2, \\ D_3 &= i(\nu - \omega_0) + \Gamma_2,\end{aligned}$$

and

$$D_4 = i(2\nu - \nu' - \omega_0) + \Gamma_2.$$

The denominators can be easily interpreted. D_2 and D_3 are, respectively, weak-and strong-field absorptions with excitation. D_1 is the extra or Rayleigh resonance which involves weak-field emission and strong-field absorption without excitation. The D_4 term is a three photon resonance which involves absorption of two strong-field photons, emission of a weak-field photon, and excitation. The $\Delta\rho_0$ factor is the two-level population difference saturated by the strong field. The B_1 terms are due to population beats at the difference frequency $\nu - \nu'$ and lead to a number of interesting effects.

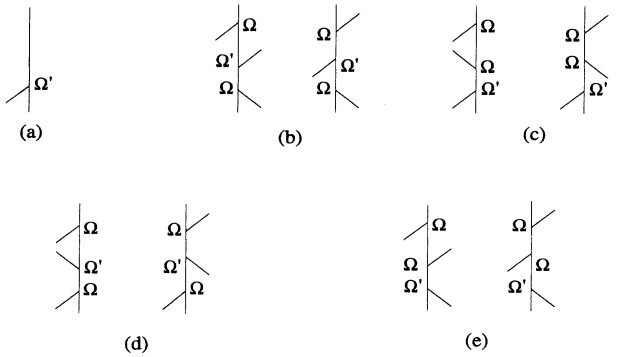

FIG. 6. The diagrams contributing to the Stokes and the four-wave mixing or anti-Stokes responses of a two-level system subjected to a strong pump at ν and a weak probe at frequency ν'. (a) First term of Eq. (50), (b) second term of Eq. (50) involving the $\frac{1}{D_3}$ propagator term in the second line of 53, (c) second term of Eq. (50) involving the $\frac{1}{D_2}$ propagator term in the second line of (53), and (d) and (e) the analogous anti-Stokes terms of Eq. (51). Only those terms involving initial ground-state population are shown. The left terms of (b)–(e) involve ground-state population beats after the second vertex and the right terms excited-state population beats.

These analytical results are displayed nicely in terms of diagrams as shown in Fig. 6. Figure 6(a) shows the basic term, which is the first term of Eq. (50). Here we show only the diagram associated with the ground state, although the initial population is self-renormalized. For the second term if B_1 is substituted from the second line of Eq. (53), one obtains four terms involving self-renormalized population beats. Two of these involve the $1/D_2$ bare propagator. These are shown in Fig. 6(b), the first giving the self-renormalized ground-state population beat after the second vertex and the second an excited-state population beat after the second vertex. These are equal if the decay rate of the excited and ground states are equal giving the factor of two in Eq. (53). Figure 6(c) shows the analogous set involving the $1/D_3$ propagator from the second line of Eq. (52). An analogous set of diagrams are obtained for the anti-Stokes terms $\rho_{21,-1}$ and are shown in Figs. 6(d) and 6(e).

E. Extra resonances

Extra or Rayleigh resonances in ρ_{12} occur at $\nu' = \nu$. This is most readily displayed with the assumption that $|\nu - \nu'| \ll |\nu - \omega_0|, |\nu' - \omega_0|$. The terms $D_1, D_2 + D_3$ and $D_2 + D_4$ in B_1 depend strongly on $\nu' - \nu$ while the remaining terms can be considered to be only functions of ν. Thus, to good approximation, $D_2 = D_3^*$, $D_4 = D_3$, and we may write

$$\frac{\Omega B_1}{\Omega'} = \frac{2|\Omega|^2}{|D_3|^2 + 4|\Omega|^2\frac{\Gamma_2}{\Gamma_1}}\left[1 + \frac{(2\Gamma_2 - \Gamma_1)|D_3|^2 + 4|\Omega|^2\Gamma_2}{[i(\nu - \nu') + \Gamma_1](|D_3|^2 + 4|\Omega|^2) + 4(\Gamma_2 - \Gamma_1)|\Omega|^2}\right]. \tag{54}$$

The extra or Rayleigh resonance vanishes when $2\Gamma_2 = \Gamma_1$ and $|D_3| \gg |\Omega|$. Since the condition on the damping constants is typically satisfied for radiative decay but not for collisions, we may say that the extra resonances are "induced" either by collisions [46] or by the presence of a strong pump field [43, 47].

F. Probe amplification

We also note that when $\Delta\rho^{(0)} = 1$ (only the ground state is initially occupied), Eq. (53) substituted into Eq. (50) gives the expression used by Wu *et al.* [48] for the analysis of their experimental studies of the Stokes gain/loss profile predicted by Mollow [49]. In their case, $2\Gamma_2 = \Gamma_1 = \Gamma$; also, their $z = D_3$ and $\delta\nu = \nu' - \nu$; furthermore, our value of $|\Omega|^2$ is defined to be four times that of Mollow and co-workers. It should be noted that the amplification process is related to the problem of "lasers without inversion" [50, 51].

Figure 7(a) shows the theoretical Stokes line shape $\mathrm{Im}\rho_{21}(\nu')$ plotted as a function of the normalized weak-field detuning $\delta\nu'/\Gamma$, where $\delta\nu' = \nu' - \omega_0$, and normalized strong-field amplitude $|\Omega|/\Gamma$ with strong field on resonance. This gives the predicted and observed profiles as is more readily apparent in the form shown in Fig. 7(b). As the intensity is increased, two dips in the weak-field absorption profile appear one on either side of line center. For a specific value of normalized strong-field amplitude the medium becomes transparent at these two

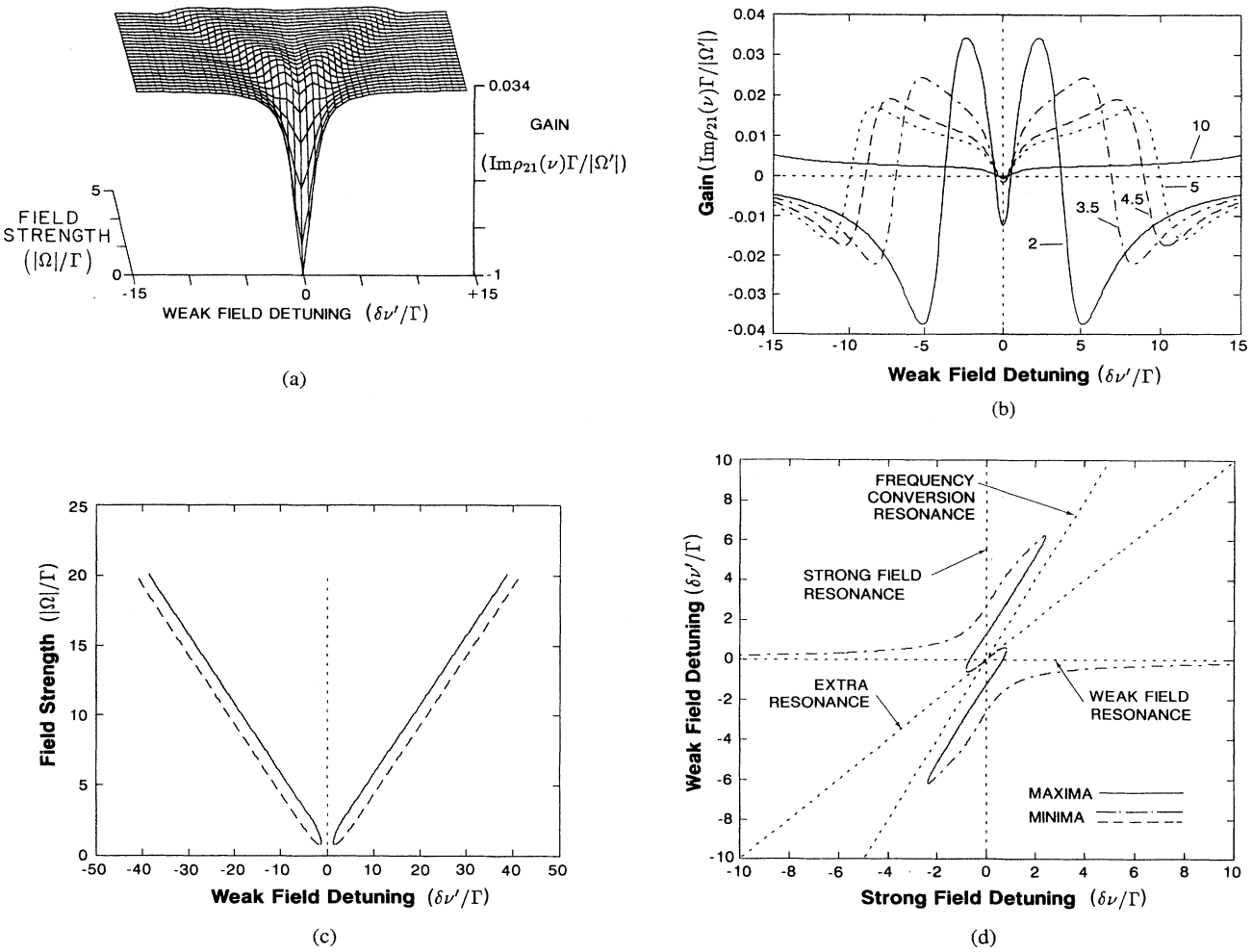

FIG. 7. Stokes line shape of a two-level system resonantly excited by a strong field. (a) Surface plot of the line shape as a function of the normalized weak-field detuning $\delta\nu'/\Gamma$ and normalized strong-field amplitude $|\Omega|/\Gamma$, respectively, with strong field on resonance. (b) Curves of $\mathrm{Im}\rho_{21}(\nu)\Gamma/|\Omega'|$ as a function of weak-field detuning for normalized strong-field amplitudes equal to $|\Omega|/\Gamma = 2$, 3.5, 4.5, 5, and 10 and strong field on resonance. (c) Plot showing the location of the maxima (solid line) and minima (dashed line) as a function of the weak-field detuning $\delta\nu'/\Gamma$ and the strong-field amplitude $|\Omega|/\Gamma$ with the strong field on resonance. (d) Trajectories of the maxima and minima in the $\delta\nu'/\Gamma$, $\delta\nu/\Gamma$ plane with the normalized strong-field magnitude $|\Omega|/\Gamma = 1.0$. Solid lines are used for the two gain peaks, and dashed and dash-dotted lines are used for the loss peaks. Also shown are lines corresponding to the real parts of D_1, D_2, D_3, and D_4 equal to zero. These are, respectively, $\delta\nu' = \delta\nu, \delta\nu' = 0, \delta\nu = 0$, and $\delta\nu' = 2\delta\nu$.

frequencies and further increase in the strong-field intensity produces gain. The locations of the maxima (solid lines) and minima (dotted and dashed lines) of $\mathrm{Im}\rho_{21}(\nu')$ are shown in Fig. 7(c) as a function of weak-field detuning $\delta\nu/\Gamma$ and strong-field amplitude $|\Omega|/\Gamma$ with strong field on resonance. For high strong-field amplitudes, the zero crossings furthest from line center are located at frequency shifts equal to the Rabi frequency, as pointed out by Wu *et al.* [49].

When the strong field is detuned as well, the two maxima and three minima shift, all except the central minimum eventually merging and disappearing. The trajectories of these extrema in the two-dimensional detuning plane are shown in Fig. 7(d) for a normalized strong-field strength of 1.0. Inversion symmetry through the origin is apparent. The two maxima (solid lines) and two outermost minima (dash-dotted lines) tend to be asymptotic to the resonance associated with $1/D_4$, the frequency conversion or three photon $\delta\nu' = 2\delta\nu$ resonance. The minimum along $\delta\nu' = \delta\nu$ (dashed lines) is the extra or Rayleigh resonance at $\nu = \nu'$ explicitly given in Eq. (54) and associated with $1/D_1$. Also indicated are the weak- and strong-field resonance lines given by the zeros of the real parts of the D_2 and D_3 denominators as discussed above.

Similar behavior is observed in the anti-Stokes polarization amplitude normalized by $|\Omega'|/\Gamma$ as shown in Fig. 8 where the normalized strong field strength is 3.6. Figure 8(a) shows the surface plot of the intensity and Fig. 8(b) the trajectories of the maxima and minima. For positive strong-field detuning maxima (solid lines) occur along the $\delta\nu' = \delta\nu$ frequency conversion line and the $\delta\nu' = 0$ weak-field resonance line, respectively. Below the critical value of the strong field for which the resonance peak is not split, the maximum along the extra resonance line disappears and only a single minimum is seen.

The theory can be modified to also include a weak-field amplitude at $2\nu - \nu'$; both ν' and $2\nu - \nu'$ can then be amplified together in a parametric process [52].

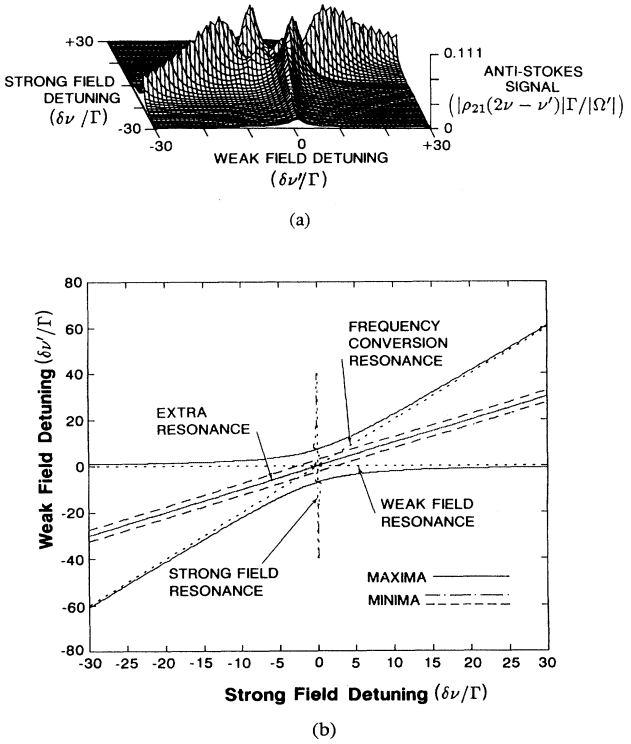

FIG. 8. Normalized anti-Stokes polarization amplitude $|\rho_{21}(2\nu - \nu')|\Gamma/|\Omega'|$ plotted as a function of the normalized weak-field detuning $\delta\nu'/\Gamma$ and the normalized strong-field detuning $\delta\nu/\Gamma$ for a value of the strong field given by $\Omega = 3.6\Gamma$. (a) Surface plot of the normalized anti-Stokes polarization amplitude plotted as a function of the weak-field and strong-field detuning, $\delta\nu'/\Gamma$ and $\delta\nu/\Gamma$, respectively. (b) Trajectories of the maxima (solid lines) and minima (dash-dotted and dashed lines) of (a) plotted as a function of normalized weak-field $\delta\nu'/\Gamma$ and strong-field detuning $\delta\nu/\Gamma$.

VII. CONCLUSION

In this paper, we have considered an alternative approach to the treatment of strong-field nonlinear optical problems. This has involved the substitution of the density matrix into itself, thereby having a coupled set of equations for which intermediate density-matrix elements are eliminated. This reduces the number of equations which need to be handled for many nonlinear optical problems by a factor of 2. In addition, we have shown that by using differences between populations of levels and reasonable approximations to the damping coefficients further simplification occurs. For example, for two strong fields we have shown that, while 128 terms occur in the original density matrix equations, the final number can be reduced to 2.

The resultant equations involve double interaction terms and contain in a concise way radiative-renormalization phenomena such as saturation, Rabi splitting, field-induced extra resonances, and other phenomena more traditionally viewed from the dressed-atom picture. We have applied this approach to obtain several two-level results including excitation by two strong fields, weak-field Stokes transparency and amplification, and anti-Stokes polarization. There are a variety of other problems which can be handled in this manner including electromagnetically induced transparency in upconversion processes, when either two or one of the pump beams has a high intensity.

The approach which we have developed here is equivalent to a Dyson-equation analysis and therefore incorporates the dressed-atom picture as well as the perturbation approach to renormalization. It is important, however, to emphasize that it is not inherently a perturbational approach.

Finally, it should be pointed out that, whereas the ap-

plications which have been considered in the present paper are semiclassical, this need not necessarily be the case. It will be interesting to explore the quantum limit for applications to vacuum-field fluctuation calculations useful for cavity QED or noise problems. In this case the paired interactions for a mode results in the photon propagator, as recently discussed [53]. As such, it is also related directly to Wick's theorem for pairing of interactions with the elimination of intermediate excitations [54].

ACKNOWLEDGMENTS

The University of California portion of this work was partially supported by the Air Force Office of Scientific Research. The Lincoln Laboratory portion of this work was sponsored by the Department of the Air Force. We would like to thank H. Bervas, S. Le Boiteux, A. E. Kaplan, J.-P. E. Taran, and B. Attal-Trétout for their useful comments and encouragement during the course of this work.

---

* Present address: Electro-Optics Technology Center, Tufts University, Medford, MA 02155.

[1] K.-J. Boller, A. Imamoğlu, and S. E. Harris, Phys. Rev. Lett. **66**, 2593 (1991).
[2] J. E. Field, K. H. Hahn, and S. E. Harris, Phys. Rev. Lett. **67**, 3062 (1991).
[3] S. E. Harris, J. E. Field, and A. Imamoğlu, Phys. Rev. Lett. **64**, 1107 (1990).
[4] T. K. Yee, Ph. D. dissertation, University of California, Berkeley, 1988.
[5] T. K. Yee and T. K. Gustafson, Phys. Rev. A **18**, 1597 (1978).
[6] Y. Prior, IEEE J. Quantum Electron. **QE-20**, 37 (1984).
[7] R. Trebino, Phys. Rev. A **38**, 2921 (1988).
[8] For an early approach to this problem, see O. Blum, I. Kim, T. K. Gustafson, P. L. Kelley, and J.-P. E. Taran, in *Technical Digest of the First Topical Conference on Nonlinear Optics: Materials, Phenomena, and Devices* (IEEE, Piscataway, NJ, 1990), paper WP9.
[9] P. L. Kelley, O. Blum, and T. K. Gustafson, in *Technical Digest of the Second Topical Conference on Nonlinear Optics: Materials, Fundamentals, and Applications*, 1992 Technical Digest Series (Optical Society of America, Washington, DC, 1992), Vol. 18, paper TUD4; P. L. Kelley, O. Blum, P. Harshman, and T. K. Gustafson (unpublished).
[10] P. Harshman, O. Blum, T. K. Gustafson, and P. L. Kelley (unpublished).
[11] S. Swain, J. Phys. B **13**, 2375 (1980).
[12] K. I. Osman and S. Swain, J Phys. B **13**, 2397 (1980).
[13] K. I. Osman and S. Swain, Phys. Rev. A **25**, 3187 (1982).
[14] F. Bloch, Phys. Rev. **70**, 460 (1946).
[15] L. Van Hove, Physica **21**, 517 (1955); **23**, 441 (1957).
[16] R. Zwanzig, J. Chem. Phys. **33**, 1338 (1960); in *Lectures in Theoretical Physics*, edited by W. E. Brittin (Interscience, New York, 1961), Vol. III, p. 106; Phys. Rev. **124**, 983 (1961).
[17] U. Fano, Phys. Rev. **131**, 259 (1963).
[18] P. N. Argyres, in *Proceedings of the Eindhoven Conference on Magnetic and Electric Resonance and Relaxation*, edited by J. Smidt (North-Holland, Amsterdam, 1963), p. 555.
[19] P. N. Argyres and P. L. Kelley, Phys. Rev. **134**, A98 (1964).
[20] C. Cohen-Tannoudji, in *Frontiers in Laser Spectroscopy*, edited by R. Balian, S. Haroche, and S. Liberman (North-Holland, Amsterdam, 1977), pp. 3–105.
[21] A. Ben-Reuven and Y. Rabin, Phys. Rev. A **19**, 2056 (1979).
[22] N. Bloembergen and Y. R. Shen, Phys. Rev. **133**, A37 (1964).
[23] S. Singh and G. S. Agarwal, J. Opt. Soc. Am. B **5**, 254 (1988).
[24] R. Kubo, Nuovo Cimento Suppl. **6**, 1071 (1957).
[25] L. I. Gudzenko and S. I. Yakovlenko, Zh. Eksp. Teor. Fiz. **62**, 1686 (1972) [Sov. Phys.—JETP **35**, 877 (1972)]; Zh. Tekh. Fiz. **45**, 234 (1975) [Sov. Phys.—Tech. Phys. **20**, 150 (1975)].
[26] C. Cohen-Tannoudji and S. Reynaud, J. Phys. B **10**, 345 (1977); **10**, 365 (1977); **10**, 2311 (1977).
[27] L. R. Wilcox and W. E. Lamb, Jr., Phys. Rev. **119**, 1915 (1960).
[28] A. M. Levine, W. M. Schreiber, and A. N. Weiszmann, Phys. Rev. A **25**, 625 (1982).
[29] A. M. Levine, N. Chencinski, W. M. Schreiber, A. N. Weiszmann, and Y. Prior, Phys. Rev. A **35**, 2550 (1987).
[30] M. S. Kumar and G. S. Agarwal, Phys. Rev. A **33**, 1817 (1986).
[31] M. Baranger, Phys. Rev. **111**, 494 (1958); **112**, 855 (1958).
[32] R. P. Feynman, F. L. Vernon, and R. W. Hellwarth, J. Appl. Phys. **28**, 49 (1957).
[33] J. Elgin, Phys. Lett. **80A**, 140 (1957).
[34] F. T. Hoie and J. H. Eberly, Phys. Rev. Lett. **47**, 838 (1981); Phys. Rev. A **25**, 2168 (1982).
[35] L. Allen and J. H. Eberly, *Optical Resonance and Two-Level Atoms* (Wiley, New York, 1975).
[36] V. S. Butylkin, A. E. Kaplan, Yu. G. Khronopulo, and E. I. Yakubovich, *Resonant Nonlinear Interactions of Light with Matter* (Springer-Verlag, Berlin, 1989).
[37] R. W. Boyd, *Nonlinear Optics* (Academic, New York, 1992), pp. 225–237.
[38] R. W. Boyd and M. Sargent III, J. Opt. Soc. Am. B **5**, 99 (1988).
[39] S. H. Autler and C. H. Townes, Phys. Rev. **100**, 703 (1955).
[40] S. Stenholm and W. E. Lamb, Jr., Phys. Rev. **181**, 618 (1969).
[41] K. Shimoda amd K. Uehara, Jpn. J. Appl. Phys. **10**, 460 (1971); K. Uehara and K. Shimoda, *ibid.* **10**, 623 (1971).
[42] G. I. Toptygina and E. E. Fradkin, Zh. Eksp. Teor. Fiz. **82**, 429 (1982) [Sov. Phys.—JETP **55**, 246 (1982)].
[43] G. S. Agarwal and N. Nayak, J. Opt. Soc. Am. B **1**, 164 (1984).
[44] E. V. Baklanov and V. P. Chebotaev, Zh. Eksp. Teor. Fiz. **60**, 552 (1971) [Sov. Phys.—JETP, **33**, 300 (1971)];

61, 922 (1972) [**34**, 490 (1972)].
[45] S. Haroche and F. Hartmann, Phys. Rev. A **6**, 1280 (1972).
[46] Y. Prior, A. R. Bogdan, M. Dagenais, and N. Bloembergen, Phys. Rev. Lett. **46**, 111 (1981); N. Bloembergen, A. R. Bogdan, and M. W. Downer, in *Laser Spectroscopy V*, edited by A. R. W. McKellar, T. Oka, and B. P. Stoicheff (Springer-Verlag, Berlin, 1981), pp. 157–165.
[47] H. Friedmann and A. D. Wilson-Gordon, Phys. Rev. A **26**, 2768 (1982).
[48] F. Y. Wu, S. Ezekiel, M. Ducloy, and B. R. Mollow, Phys. Rev. Lett. **38**, 1077 (1977).
[49] B. R. Mollow, Phys. Rev. A **5**, 2217 (1972).
[50] D. Grandclément, G. Grynberg, and M. Pinard, Phys. Rev. Lett. **59**, 40 (1987); **59**, 44 (1987).
[51] A. Lezema, Y. Zhu, M. Kanskar, and T. W. Mossberg, Phys. Rev. A **41**, 1576 (1990).
[52] R. W. Boyd, M. G. Raymer, P. Narum, and D. J. Harter, Phys. Rev. A **24**, 411 (1981).
[53] T.K. Gustafson, J. IEEE Quantum Electron. **QE-25**, 2179 (1989).
[54] F. Mandel and G. Shaw, *Quantum Field Theory* (Wiley-Interscience, New York, 1984), pp. 102–106.